https://doi.org/10.5194/se-2020-23
Preprint. Discussion started: 9 March 2020

Solid Earth Discussions

Influence of inherited structural domains and their particular strain distributions on the Roer Valley Graben evolution from inversion to extension

Jef Deckers[1], Bernd Rombaut[1], Koen Van Noten[2] and Kris Vanneste[2]

1: VITO, Flemish Institute for Technological Research, Boeretang 200, BE-2400 Mol, Belgium
2: Seismology-Gravimetry, Royal Observatory of Belgium, Ringlaan 3, BE-1180 Brussels, Belgium

ABSTRACT:
After their first development in the middle Mesozoic, the overall NW-SE striking border fault systems of the Roer Valley Graben were reactivated as reverse faults under Late Cretaceous compression (inversion) and reactivated again as normal faults under Cenozoic extension. In Flanders (northern Belgium), a new geological model was created for the western border fault system of the Roer Valley Graben. After carefully evaluating the new geological model, this study shows the presence of two structural domains in this fault system with distinctly different strain distributions during both Late Cretaceous compression and Cenozoic extension. A southern domain is characterized by narrow (< 3 km) localized faulting, while the northern is characterized by wide (>10 km) distributed faulting. The total normal and reverse throw in the two domains was estimated to be similar during both tectonic phases. The repeated similarities in strain distribution during both compression and extension stresses the importance of inherited structural domains on the inversion/rifting kinematics besides more obvious factors such as stress directions.
The faults in both domains strike NW-SE, but the change in geometry between them takes place across the oblique WNW-ESE striking Grote Brogel fault.
Also in other parts of the Roer Valley Graben, WNW-ESE striking faults are associated with major geometrical changes (left-stepping patterns) in its border fault system. This study thereby demonstrates the presence of different long-lived structural domains in the Roer Valley Graben, each having their particular strain distributions that are related to the presence of non-colinear faults.

1. Introduction

Under Late Cretaceous compression, a large number of middle Mesozoic rift basins in West- and Central Europe was inverted, mainly by reverse reactivation of their bounding faults (de Jager, 2003; Kockel, 2003). Contrary to most of the other rift basins, after Late Cretaceous inversion, the Roer Valley Graben (RVG) experienced differential subsidence again from the late Oligocene onwards (Demyttenaere, 1989; Geluk et al., 1994). The RVG thus forms a key area to study the kinematics of repeated reactivation of graben border faults under both compression and extension.
The RVG border faults are dominantly NW-SE oriented, and locally intersected by WNW-ESE striking faults (Michon et al., 2003; Worum et al., 2005). Some of the largest WNW-ESE striking faults (such as the Grote Brogel, Lövenicher-Kast and Veldhoven faults) caused major left-stepping patterns in the overall NW-SE graben border geometry during both compression and extension. This is indicated by gravimetric maps of the area (Fig. 1) and in more detail in geological maps of both the middle Mesozoic (Jurassic), Upper Cretaceous and Cenozoic stratigraphic distributions of the area (c.f. Duin et al., 2006; Deckers et al., 2019). The influence of the interaction between the NW-SE and WNW-ESE striking faults on the structural development of the RVG during either inversion or extension has, however, never been studied in detail. By doing so, this study aims at a better understanding of the influence of non-colinear (i.e. not in line) faults on different episodes of graben border reactivation.

For site location, we selected the western border fault system of the RVG (Fig. 1), which in Belgium is characterized by long NW-SE faults (such as the Bocholt, Neeroeteren, Reppel and Rotem faults) and the major WNW-ESE oriented Grote Brogel fault (GBF). The Quaternary activity of the GBF and its influence on the local hydrology was recently studied at two investigation sites by means of

https://doi.org/10.5194/se-2020-23
Preprint. Discussion started: 9 March 2020

Solid Earth Discussions

shallow boreholes, Cone Penetration Tests, electrical resistivity tomography measurements and topographic maps by Deckers et al. (2018). To analyze the interaction of the GBF with the other faults in the western RVG and its influence on the large-scale graben geometry, we used recently published data of the 3D Geological Model for Flanders (version 3; G3Dv3-model; Deckers et al., 2019) together with topographic maps. The G3Dv3-model of the area was created by the integration of all available seismic and borehole data. It consists, among others, of layer maps for over hundred stratigraphic units ranging from the Quaternary at the surface up to the Lower Paleozoic basement at depths of almost 10 km. The layer maps illustrate the Late Cretaceous and Cenozoic stratigraphic distributions with respect to the faults. Evaluating these maps allows reconstructing the geometrical changes of the study area through time.

2. Geological setting and stratigraphy

The RVG probably developed into a rift basin during Jurassic and/or early Cretaceous regional extension (Cimmerian phases in Fig. 2; Geluk et al., 1994). This development coincided with the activity along a large number of predominantly NW-SE and WNW-ESE striking faults across the area (Worum et al., 2005). During subsequent Late Cretaceous compression, referred to as the Sub-Hercynian phase, the Campine Block (CB) and Peel Block experienced subsidence with the deposition of generally between 200 and 300 m of carbonates of the Chalk Group, while the RVG in between them was squeezed upwards or inverted (Geluk et al., 1994; Fig. 2). Inversion of the RVG took place by reverse movements along its (pre-existing) border faults (Demyttenaere, 1989). Apatite fission track analyses revealed that the amount of late Cretaceous uplift of the RVG is remarkably similar to the amount of subsidence of its flanks (Luijendijk et al., 2011).

By late Maastrichtian times, inversion of the RVG had ended and the entire region was subsequently covered by the youngest (generally < 80 m thick) sequences of the Chalk Group (Demyttenaere, 1989). For the purpose of this study, these late Maastrichtian and Danian sequences will not be included in the Chalk Group. Our informal definition of the Chalk Group thereby only contains those parts of the Chalk Group that were deposited during inversion of the RVG, and are therefore missing inside the RVG.

From the early Cenozoic onwards, the study area was situated in the southern part of the North Sea Basin and covered by several 100 meters of siliciclastics (Fig. 2). Some tectonic phases did occur in between the start of the Paleogene and the end of the early Oligocene (Fig. 2), but without major fault activity (c.f. Deckers & Van der Voet; 2018). For the purpose of this study, the late Maastrichtian to early Oligocene strata are referred to as the Cenozoic pre-rift strata.

Major fault activity resumed in the late Oligocene, when the Roer Valley Rift System developed as a northwest-trending branch of the Rhine-Graben-System (Ziegler, 1988), throughout the south-eastern part of the Netherlands, the north-eastern part of Belgium and adjacent parts of Germany (Fig. 1). This system currently extends over a distance of roughly 200 km and has a width of up to 75 km. The main faults or those with the strongest displacements divide the central Roer Valley Rift System into the CB in the west, the RVG in the center and Peel Block in the east. The Roer Valley Rift System is currently still active as indicated by the earthquake activity in the region (Fig. 1). Syn-rift sedimentation started with the deposition of the late Oligocene Voort Formation (base syn-rift strata in this study). After the Oligocene, sedimentation gradually coarsened from shallow to marginal marine glauconitic sands (Bolderberg and Diest formations) until the end of the Miocene, to coarser marginal marine to fluvial sands in the Pliocene (Mol and Kieseloolite formations) and gravel-bearing fluvial sands in the Quaternary (Meuse Group). Due to the relatively strong resistance to erosion of the gravel-bearing sands of the Meuse Group, the easternmost part of the Campine Block is currently a relatively high area (often referred to as the Campine Plateau; Fig. 3) delimited to the west by the deposition limit of these coarse sediments and in the east by the major border faults of the RVG (Beerten et al., 2013), which separate the Campine Plateau from the Reppel, Kaulille and Bocholt

https://doi.org/10.5194/se-2020-23
Preprint. Discussion started: 9 March 2020

Plains (Paulissen, 1997, Fig. 3). As a result of continuous rifting since the late Oligocene, the abovementioned stratigraphic units are relatively thick in the RVG (over 1000 m) compared to the flanking CB and Peel Blocks (generally below 500 m; Demyttenaere, 1989; Geluk, 1990).
During Miocene to recent rifting, fault distribution in the Roer Valley Rift System was characterized by two main trends: the dominant NW-SE (N145-160) trend corresponding to the general orientation of the graben, and the secondary WNW-ESE (N110-120) oblique orientation (Michon et al., 2003). These directions were both favorable for fault reactivation under the NE-SW Miocene to recent extensional direction (Michon et al., 2003; Michon & Van Balen, 2005). Along its eastern border, the RVG is separated from the Peel Block by the Peel Boundary fault zone, a NW-SE oriented, 100 km long narrow deformation zone composed of the Peel boundary fault and several secondary faults (Michon & Van Balen, 2005) with a total vertical throw of 400-800 m for the base of the Miocene (Geluk et al., 1994). Along its western border, the RVG is separated from the CB by a broad fault bundle, the Feldbiss fault system (FFS), which consists of a number of faults showing a left-stepping pattern. As a result of this left-stepping pattern, the RVG changes from a near full graben in the center to an asymmetric graben in the north (Michon & Van Balen, 2005). The FFS is 80 km long and is mainly composed of the Feldbiss fault, the Geleen (NL) or Neeroeteren (BE) fault and the Heerlerheide (NL) or Rotem (BE) fault (Michon & Van Balen, 2005; Fig. 3) and shows vertical throws of the base of the Miocene of roughly 400 m (Demyttenaere & Laga, 1988). The stratigraphic thicknesses indicate that the Peel Boundary fault system was generally more active than the FFS since the beginning of the Miocene (Michon & Van Balen, 2005). Consequently, the main Miocene to recent depocenters developed in the hangingwall of the Peel Boundary fault system.
The study area is centered on the GBF, which is situated in the central portion of the FFS (Fig. 1). The GBF branches off from the major Neeroeteren fault in a WNW-ESE orientation. It has a pronounced scarp (up to 4m) in the geomorphology which gradually fades away towards the west (Fig. 3). This gradual disappearance coincides with the decrease in fault throw of the Pleistocene Meuse terraces (Deckers et al., 2018).

3. Dataset and methodology

3.1 General dataset

In the past two decades, a large number of (hydro)geological models have been created for the study area (c.f. Langenaeker, 2000; Sels et al., 2001; Beerten et al., 2005; Meyus et al., 2005; Matthijs et al., 2013; Deckers et al., 2019) or parts of it (Deckers et al., 2014; Vernes et al., 2018). For the purpose of this study, we rely on the most recently published 3D subsurface model of Flanders (northern part of the Belgium), called the G3Dv3-model (Deckers et al., 2019). This model consists of 3D models of over hundred lithostratigraphic units from the Lower Paleozoic (at depths of up to 10 km) up to the Quaternary at the surface. The G3Dv3-model also contains 3D surfaces of over two-hundred faults in the eastern part of Flanders. For the eastern border region between Flanders and the Netherlands, the 3D(hydro)geological models of the Cenozoic stemming from two cross-boundary projects, namely the H3O-Roer Valley Graben and H3O-Campine area (Deckers et al., 2014; Vernes et al., 2018), were integrated and stratigraphically further detailed/updated in the G3Dv3-model. Consequently, the G3Dv3-model combines the most recent geological knowledge in Flanders.

The main data sources to create the G3Dv3-model were the following:

- Boreholes: Several tens of thousands of borehole descriptions from Flanders are present in the databases of DOV ("Database subsoil Flanders"; https://www.dov.vlaanderen.be/) and of the Geological Survey of Belgium. Besides the descriptions, these databases often contain one or more interpretations of the lithostratigraphic successions (groups, formations, members) in each borehole. Thousands of these interpretations were selected from these databases as a starting point to create the geological models. After selection, the existing lithostratigraphic interpretations of the boreholes were critically examined and accepted, rejected or reinterpreted for the different stratigraphic layers. An overview on the used boreholes to map the Chalk Group, base syn-rift strata and base Quaternary and Pliocene strata is shown in figure 4.

- Seismic data: The eastern part of Flanders is covered by over 400 lines from numerous seismic campaigns that were performed between 1953 and 2015. This dataset consists of more widely spaced seismic lines from a regional seismic survey performed between 1953-1956 (Campine Basin), complemented by dense networks of more closely spaced lines from local surveys mainly conducted between the 1980's and 2015. In general, the quality of the seismic data improves with time. Besides the age, also the targeted depth-range of the seismic survey strongly influences the vertical resolution of the seismic data. Some seismic surveys target deep (> 2 km) Lower Carboniferous strata, while others target shallow (< 1 km) Cenozoic strata. Consequently, the quality of the resulting image is better for the deep and shallow range, respectively. The entire selection of seismic lines was interpreted for horizon and fault mapping. An overview on the interpreted seismic lines to map the Chalk Group and base syn-rift strata is shown in figure 4.
- Topographic data: The Digital Terrain Model forms the top of the G3Dv3-model. As a result of their recent activity, several of the large RVG boundary faults are expressed in the topography by relief gradients or scarps (Camelbeeck & Meghraoui, 1996; Paulissen, 1997; Fig. 3). The relief gradient provides a good indication of the location and orientation of the fault traces of these boundary faults at the surface, especially when used in combination with the seismic data.

3.2 Dataset in the study area

The dataset used to analyse the study area is limited to a horizontal (area around the GBF) and vertical (depth interval corresponding to Upper Cretaceous and Cenozoic) subset of the G3Dv3-model. Because of this restriction the following data-selection was made:

Stratigraphic layers:

- The top, base and thickness of the Upper Cretaceous syn-inversion strata of the Chalk Group were selected, since they illustrate the inversion-related (Late Cretaceous) deformation. The top and base of the Chalk Group were mainly based on seismic interpretations, locally supported by borehole interpretations (for location, see Fig. 4). Boreholes and seismic data show that the Chalk Group is absent within the RVG, and up to 300 m thick in the CB.
- The bases of the syn-rift (Voort Formation) and Pliocene to Quaternary strata (equivalent Mol/Kieseloolite Formations) were selected to illustrate the Cenozoic extension-related deformation. The model of the base syn-rift strata was mainly based on seismic interpretations either from this horizon itself or from a nearby horizon, and supported by borehole interpretations (for location, see Fig. 4). The base of the Pliocene to Quaternary strata is generally too shallow to be consistently seismically interpreted, and was therefore solely based on borehole interpretations (for location, see Fig. 4). Due to the shallow location, the number of available boreholes for the Pliocene to Quaternary strata was high compared to those available to map the underlying layers (compare in Fig. 4).

Faults:

From the sets of faults in the G3Dv3-models in the study area, we only selected those that show an offset in the Chalk Group and in the base of the syn-rift strata (for location, see Fig. 4).
Due to the relatively large spacing between the boreholes, predominantly seismic data were used for fault mapping. Since all of the used seismic data are two-dimensional, only fault lines are imaged and their lateral connection into one fault plane remains interpretative. The long faults discussed in this study should therefore not be considered as single fault planes, but rather as fault systems, each

https://doi.org/10.5194/se-2020-23
Preprint. Discussion started: 9 March 2020

of which represents one tectonic feature made up by different fault lines that can represent either linked or isolated fault segments (following Rypens et al., 2004). The interpreted lateral connection of the 2D fault lines into 3D fault systems was predominantly based on the comparison of the variation of vertical displacements between adjacent seismic profiles, locally supported by topographic indications and borehole data. The most reliable fault models are therefore created from areas with low structural complexity, high seismic coverage, large numbers of boreholes and strong topographic relief of the faults.

2D seismic coverage is generally high for the area south of the village of Bree because of the dense networks of different seismic surveys across the RVG border fault system (Fig. 4). The seismic interpretations and lateral connections of the border faults (such as the Bree, Dilsen, Neeroeteren and Rotem faults) are therefore most reliable in this area. In addition, the major Neeroeteren fault is clearly expressed in the topography as a large (+/- 30m) relief gradient, often referred to as the Bree Fault Scarp (Camelbeeck & Meghraoui, 1996; Fig. 3).
North of the village of Bree, on the other hand, 2D seismic coverage is very poor with only five long, low to average quality seismic lines (either old or only imaging the Cenozoic; Fig. 4). Consequently, interpreting faults and their lateral connections in the RVG border zone on seismic data alone would have a high degree of uncertainty. The southern sections of the Bocholt, GBF and Reppel faults are, however, clearly expressed by topographic gradients (Fig. 3), which provide support for the seismic fault line connections. At locations where the topographic expression fades, however, the uncertainty increases again:

- In its eastern portion, the GBF is clearly expressed by a topographic gradient of over 10 m with a clear fault scarp up to 4 m high near Bree (Deckers et al., 2018; Fig. 3). As its throw decreases in western direction, however, its topographic expression fades, which causes a major uncertainty (of several km's) on the exact location and extent of the northwestern tip of the GBF.
- In the western portion of the GBF, Demyttenaere & Laga (1988) interpreted an important bend towards the NW-SE Overpelt fault (Fig. 4). The topographic expression is, however, too faint to corroborate this bend in the GBF (Fig. 3). A recently reprocessed seismic line nearby also shows only a minor throw near the location of the supposed bend (question mark on Fig. 4). So although this bend of the GBF towards the Overpelt fault is indicated as a major fault in geological models, its importance remains largely uncertain and is therefore indicated on figures 4, 5 and 6 with question marks. Contrary to the bend of the GBF, the presence of the Overpelt fault is supported by several seismic lines (Fig. 4). The Overpelt fault runs more or less parallel to the Reppel and Bocholt-Hamont faults further east.
- Due to the lack of clear topographic expression of faults and due to the diffuse seismic coverage, a large uncertainty remains on fault interpretations in the area between the Overpelt fault and the Rauw fault 14 km further west. West of the Rauw fault, the seismic coverage increases again and the uncertainty on fault interpretations and their lateral connection decreases.

3.3 Methodology

To illustrate the Cenozoic syn-rift kinematics in the study area, we constructed a map view of the depth of the base of the syn-rift strata and the faults that affect it (Fig. 5). Another map view was created for the thickness of the Chalk Group and the major faults that are known to have influenced it (Fig. 6) in order to illustrate the Late Cretaceous syn-compressional kinematics.
Besides the map views, also four cross-sections (Figs. 7A to -D) were constructed to illustrate the Late Cretaceous to recent sediment thicknesses and geometries in the study area. Three cross-sections are SW-NE oriented, perpendicular to the graben trend (7A, -B and -C) and another SE-NW oriented, sub-parallel to the graben trend (7D). On these cross-sections, the top and base of the

https://doi.org/10.5194/se-2020-23
Preprint. Discussion started: 9 March 2020

Chalk Group and Cenozoic pre-rift strata are indicated. The syn-rift strata are shown in two parts, namely the late Oligocene and Miocene below and the Pliocene to Quaternary on top.

4. Results

4.1 Late Oligocene to recent rifting

In the RVG, the base of the syn-rift strata is currently situated in the subsurface at depths that generally exceed -900 m TAW (Tweede Algemene Waterpassing; Fig. 5). In the CB, the base of the syn-rift strata is located at more shallow depths, ranging from at +50 m TAW in the southwest up to -400 m TAW in the northeast. Towards the easternmost parts of the CB, this trend becomes progressively more disturbed by the presence of faults and tilted blocks in the footwall domain of the FFS. For individual faults in the CB, the vertical throws at the level of the base of the syn-rift strata do not exceed 80 m.

At the FFS, the base of the syn-rift strata drops by 500 m from the CB into the RVG (from -400 m TAW to -900 m TAW; Fig. 5). This jump takes mainly place by - often large - vertical throws along a dense, complex network of normal faults of the FFS, and in between those also by an eastward dip of the syn-rift strata. Several faults in the FFS have vertical throws of the base of the syn-rift strata of over 150 m (Bocholt, GBF, Hamont, Overpelt, Reppel, Rotem), with a maximum of 500 m along the Neeroeteren fault (Figs. 7A and -B).

In the RVG itself, vertical fault throws are larger than in the CB, but smaller than in the FFS as they generally do not exceed 150 m. Most of the intra-graben faults are dipping in the direction of the nearest graben border fault system (i.e. are antithetic; Figs. 7A and -B). The simultaneous activity of the synthetic graben border faults and the antithetic intra-graben faults resulted in a series of long grabens in the western flank of the RVG (Fig. 5; Deckers, 2016).

The geometry of the FFS shows strong lateral changes across the study area. Within the FFS, two structural domains and their particular geometry were identified, north and south of the village of Bree (for location, see Fig. 3):

- The southern domain consists of the NW-SE Neeroeteren and Rotem faults (Fig. 5). The width of this domain is limited to the Neeroeteren fault in the north, and from the branching point of the Rotem fault onwards increasing in southern direction up to a maximum of 2 km near the Belgian/Dutch border. Most of the vertical throw of the FFS is taken by the NW-SE striking Neeroeteren fault, with vertical throws of the base of the syn-rift strata of almost 600 m (Figs. 7A- and B). The Rotem fault shows a maximum vertical throw of the base of the syn-rift strata of 150 m (Fig. 7A). The large vertical throw along the Neeroeteren fault is also expressed by a strong relief gradient denoted as the Bree Fault Scarp on top of this fault (topographic offset between 15-20 m; Fig. 3). This relief gradient coincides with the boundary between the elevated (> 50 m TAW) Campine Plateau on top of the CB and the low-lying (< 40 m TAW) Bocholt Plain on top of the RVG (c.f. Paulissen, 1997; Fig. 3). The relief gradient of the Bree Fault Scarp is evident between Bree and the hamlet of Waterloos, but abruptly disappears south of Waterloos due to the WSW-ENE incision by the Quaternary Meuse river from the late Pleistocene onwards (Fig. 3).

- The northern domain starts where the Neeroeteren fault bifurcates into the GBF towards the west and the Bocholt fault towards the north (Fig. 5). These two faults define the boundaries of the northern domain of the FFS. Since the GBF and Bocholt faults have a WNW-ESE and NW-SE strike respectively, the northern domain progressively widens in northern direction, reaching a width of up to 13 km in the central part (Fig. 7C). As it bifurcates, the large vertical throw along the Neeroeteren fault (almost 600 m) is roughly equally divided over the GBF and Bocholt faults (each about 250 m; Fig. 5). These values of

https://doi.org/10.5194/se-2020-23
Preprint. Discussion started: 9 March 2020

about 250 m of vertical throw are the maximum for the northern domain. As a result, while the southern domain delimits a high footwall area in the west from a low hangingwall area in the east, the northern domain shows a more gradual downfaulting in eastern direction, with relatively small throws across some of its major faults (Fig. 5). The smaller vertical throws along faults in the northern domain is also expressed by absent or only very small relief gradients for most of its faults (excluding the GBF; Fig. 3). As one of the most important faults, the Bocholt fault for example shows a vertical topographic offset of maximum 4 m near the town of Bree where the fault is only expressed as a low angle linear slope without a clear scarp. Consequently, while the Bocholt Plain and Campine Plateau are clearly delimited by the Bree Fault Scarp in the southern domain, their transition is much more stepwise along smaller fault scarps in the northern domain (Fig. 3). This stepwise topography has led to the subdivision of the Lommel, Reppel and Kaulille Plains in the northern domain of the FFS and its hangingwall (Paulissen, 1997; Fig. 3). The GBF forms the boundary between the elevated Campine Plateau and the lower Reppel and Kaulille Plains and consequently has a large topographic relief in respect to the NW-SE striking faults in the northern domain. This topographic relief is largest in the east (15-20 m) where it seems to be in continuation with the Bree Fault Scarp associated with the Neeroeteren fault (Deckers et al., 2018). As the total vertical throw along the GBF decreases in western direction, its relief gradient also decreases (Fig. 3). This decrease is, however, not gradual. Deckers et al. (2018) noticed an abrupt decrease in the topographic throw at about 2 km west of the eastern tip of the GBF. These authors related this decrease to the Reppel fault branching off from the GBF, taking over part of the total displacement (Fig. 3). Also at depth the large vertical throw of the base of the syn-rift strata along the GBF (250 m) abruptly decreases (towards 150 m) across the contact point with the Reppel fault (Fig. 5). This decrease in vertical throw (100 m) along the GBF is completely accommodated by the Reppel fault. West of the bifurcation with the Reppel fault, vertical throw along the GBF is around 100 m.

As mentioned above, at the western tip of the GBF, several authors have previously suggested a bend towards the NW-SE Overpelt fault (Demyttenaere & Laga, 1988; Broothaers et al., 2012; Deckers et al., 2015). What is clear from the seismic data is the presence of the NW-SE striking Overpelt fault further north with vertical throws in the order of 100 m (Fig. 5). Northwest of the village of Peer, however, the topographic expression of the GBF becomes faint and there is no further data (borehole nor seismic) to provide indications on its westward continuation. The decrease of topographic relief in north-western direction coincides with the decrease of vertical throw of the syn-rift strata along the large faults in the northern domain. Subsidence from the CB towards the RVG is still partly accommodated by small faults but increasingly by a strong northeastward dip of the base of the syn-rift strata (Fig. 7C).

Within the hanging- and footwall of the FFS, the boundary between the southern and northern domain of the FFS doesn't coincide with any major changes in thickness of the syn-rift strata (Fig. 5). This shows that the total throw of the FFS doesn't change across the boundary between both domains.

4.2 Late Cretaceous compression

Under Late Cretaceous compression, the CB and Peel Blocks were downthrown, while the RVG in between them was pushed upwards or inverted. Consequently, the late Cretaceous Chalk Group is absent on top of the RVG and currently up to 300 m thick within the CB (Fig. 6). Uplift of the RVG was accommodated by reverse movements along its border faults, i.e. the FFS in the west. The total amount of uplift along the FFS can therefore be estimated at over 300 m (taking into account later

https://doi.org/10.5194/se-2020-23
Preprint. Discussion started: 9 March 2020

compaction of the chalks), which is consistent with the range (250 to 500 m) obtained from apatite fission track measurements by Luijendijk et al. (2011) in the nearby borehole Nederweert.
Due to Cenozoic normal reactivation, only few faults in the study area have net reverse throws as the result of Late Cretaceous compression. These faults (Bree and Dilsen faults) are all located in the FFS (Figs. 6, 7A and 7B). The amount of reverse movements across structural features can - even for those that were later on normally reactivated - be reconstructed by studying the changing thicknesses of the Chalk Group across them. However, when the Chalk Group is absent, we are unable to quantify these reverse movements. This is the case for faults within the RVG and for the eastern (most graben-inward) section of the FFS, such as the Bocholt, Hamont and Reppel faults, but also parts of the Neeroeteren fault (Fig. 6). Therefore, only reverse movements of the westernmost faults within the FFS can be reconstructed.
The thickness maps of the Chalk Group indicate different structural patterns of uplift across the western faults of the FFS. Similar to the Cenozoic (section 4.1), these differences can be separated geographically into a southern and northern domain:

- In the part of the CB south of the town of Bree, the thickness of the Chalk Group generally increases in the direction of the RVG to reach a maximum of almost 300 m in the footwall of the FFS (Fig. 6). From this footwall, the Chalk Group strongly thins across reverse faults. Three major reverse faults were observed, namely the Bree, Rotem and Dilsen faults. The Chalk Group has a thickness of 250 m in the footwall of these faults, becoming less than 150 m thick in the hangingwall of the Dilsen fault (Fig. 7A), and very thin or even absent in the hangingwall of the Bree and Rotem faults (Fig. 7A and 7B). This shows that vertical reverse throws along faults reached 100 to 250 m or more. Since the Bree and Dilsen faults are present in the footwalls of the more important Neeroeteren and Rotem faults, and converge towards the latter faults in the Palaeozoic basement, they may represent footwall shortcut faults. The Bree and Dilsen faults would thereby have originated during Late Cretaceous compression to accommodate inversion on the pre-existing Neeroeteren and Rotem faults.
- North of Bree, from the Rauw fault onwards, the Chalk Group thins in eastern direction until it becomes absent near the Overpelt fault (Fig. 7C). East of the Overpelt fault, the Chalk Group is absent and reverse fault throws are unknown. The zone along which the Chalk Group thins is therefore at least 10 km wide. Contrary to the southern domain, thinning of the Chalk Group is not very abrupt across major reverse faults or thrust faults in the northern domain. Instead, it takes place by small reverse displacements along faults and predominantly by upwards flexuration (see flexures at the top and bottom of the Chalk Group in Fig. 7C) towards the northeast.

The transition between the southern and northern domains is located at or along the lateral extent of the GBF (Fig. 7D). The GBF thereby shows a reverse throw at the stratigraphic level of the Chalk Group of around 200 m. This throw decreases in western direction along the sections of the GBF (Fig. 6). Northwest of the western tip of the GBF, northwards thinning of the Chalk Group takes mainly place by upwards flexuration of the basement (Fig. 7C).

5. Discussion and conclusions

The western border fault system of the RVG, here referred to as FFS, probably formed in the middle Mesozoic, and was reactivated under Late Cretaceous compression and again under Cenozoic extension (Demyttenaere, 1989). Based on the new 3D geological model of Flanders (G3Dv3-model; Deckers et al., 2019), we identified two structural domains in the FFS with markedly different geometries, which existed during both Late Cretaceous compression and late Oligocene to recent extension.

- In the southern domain, the FFS is characterized by a narrow (< 2 km) border fault zone that is dominated by localized faulting. During the Late Cretaceous compression, this zone

https://doi.org/10.5194/se-2020-23
Preprint. Discussion started: 9 March 2020

was dominated by several faults with reverse throws of over 200 m, and during Cenozoic extension by the large Neeroeteren fault with a normal throw of over 500 m.

- In the northern domain, the FFS is characterized by a wide (average >10 km) border fault zone that is dominated by distributed faulting. During the Late Cretaceous compression this zone was characterized by upwards flexuring of the basement and faults with generally small reverse throws, and during Cenozoic extension by downwards flexuring of the pre-rift strata and faults with total throws of less than 250 m.

Fault domains that showed the highest Late Cretaceous contractional throw thus also showed the highest normal throws during later (Cenozoic) extension. Mora et al. (2008) showed that for the Eastern Cordillera of Colombia the same is true for faults that have been reactivated in the opposite way. In the latter area, the width of deformation, the degree of shortening, the spatial development of structures, and the focus of ongoing tectonic activity seemed to be fundamentally influenced by the inherited structures (Mora et al., 2006). The similarity of the geometry of the different domains of the FFS during both Late Cretaceous inversion and Cenozoic extension shows that inherited structures also controlled the evolution of the border zone of the RVG. This shows the importance of pre-existing structural domains on tectonic deformation during both inversion and extension, besides more obvious factors such as the fault strikes with respect to the stress-field orientations.
Within different domains, not all of the individual pre-existing faults were reactivated. The Bree and Dilsen faults (Figs. 7A and -B), for example, are very important Late Cretaceous faults in the footwalls of the Neeroeteren and Rotem faults that were not reactivated during the Cenozoic. These faults might, however, represent footwall shortcuts to accommodate inversion of the larger Neeroeteren and Rotem faults, causing them to be less prone for normal reactivation. The presence of footwall shortcut thrusts is indeed characteristic for the early stages of inversion of extensional fault systems (McClay & Buchanan, 1992).

The abovementioned geometrical changes in the FFS had no influence on its total Cenozoic vertical throw, which remains in the order of 600 m across both domains. They also seem to have had little effect upon the thicknesses of the Upper Cretaceous Chalk Group, which remains in the order of 250-300 m across the footwall of both domains of the FFS. This shows that a similar amount of strain (extensional and compressional) was distributed differently between the southern and northern domains of the FFS, namely localized in the first and distributed in the latter. Localized and distributed regimes of faulting are known to have occurred within one fault system (Soliva and Schultz, 2008; Nixon et al., 2014), similar to the FFS in this study. Differences between these regimes are often attributed to the maturity of the fault systems (Nixon et al., 2014): highly mature systems are linked and have localized strain, whereas younger (less mature) faults are less linked and more diffuse. In our study area, however, the difference in strain localization cannot be related to differences in maturity, since the FFS is a long-lived system, already active since the middle Mesozoic. Alternatively, such as is the case in the East African Rift System, the difference in fault localization could be attributed to the presence of magmatic intrusions (Ebinger and Casey, 2001; Kendall et al., 2005; Wright et al., 2006) or oblique pre-existing shear zones (Katumwehe et al., 2015; Dawson et al., 2018). The RVG is, however, considered amagmatic during the Late Cretaceous and Cenozoic and pre-existing shear zones are not known at the junction between the two domains. Instead of fault maturity, the different strain distribution is likely related to the large GBF which forms the boundary between the two abovementioned structural domains. As an inherited, oblique (WNW-ESE striking) fault in an otherwise NW-SE strike dominated fault system, the GBF caused a major left-stepping pattern in the FFS. It transitions the FFS from localized faulting in the narrow border zone to its south towards distributed faulting in a wide border zone to its north. The GBF thereby redistributes strain from one domain into the other, as indicated by the following observations:

- As the Neeroeteren fault branches into the GBF and Bocholt faults, the total throw of the Neeroeteren Fault is divided between the last two faults.

- At the bifurcation between the GBF and Reppel faults, the total throw of the GBF also decreases by an amount equal to the throw of the Reppel Fault.
- At the location where the GBF dies out, no more large displacement faults were observed in the northern domain.

This study therefore shows that the presence of a non-colinear fault enables major changes in strain distribution along graben border faults systems. North and south of the study area, other major WNW-ESE striking faults, such as the Veldhoven and Lövenicher faults (see Fig. 1 for their locations), are associated with similar left-stepping patterns and even larger geometrical changes in the border faults systems of the Cenozoic Roer Valley Rift System. Geological maps of the thickness of the Chalk Group in the Netherlands (Duin et al., 2006) illustrate that the Veldhoven fault, just like the GBF, was also already of major importance during the Late Cretaceous inversion of the RVG. The influence of non-colinear faults on the graben geometry can therefore not only be major during one tectonic phase, but be long-lived, under phases of both compression and extension.

Acknowledgements

We gratefully acknowledge financial support from the Bureau for Environment and Spatial Development - Flanders. We would like to thank K. van Baelen for her work on the figures.

References

Beerten, K., De Craen, M., and Wouters, L., 2013. Patterns and estimates of post-Rupelian erosion in the Campine area, north-eastern Belgium. Phys. Chem. Earth, 64, 12–20.

Beerten, K., Vandenberghe, N., Gullentops, F., and Paulissen, E., 2005. Toelichting bij de Quartairgeologische Kaart - kaartblad 10–18, Maaseik. In: Vlaamse overheid, dienst Natuurlijke Rijkdommen, 48 pp.

Broothaers, M., Deckers, J., Lagrou, D., and Matthijs, J. 2012) 3D-lagenmodel van de Tertiaire afzettingen in de Roerdalslenk in Vlaanderen. VITO-rapport, 2012/SCT/R/191, 58 pp.

Camelbeeck, T., and Meghraoui, M., 1996. Large earthquakes in northern Europe more likely than once thought. Eos. Trans. AGU, 77, 405-409.

Dawson, S.M., Laó-Dávila, D.A., Atekwana, E.A., and Abdelsalam, M.G., 2018. The influence of the Precambrian Mughese Shear Zone structures on strain accommodation in the northern Malawi Rift. Tectonophysics, 722, 53-68.

Deckers, J., 2016. The Late Oligocene to Early Miocene early evolution of rifting in the south-western part of the Roer Valley Graben. International Journal of Earth Sciences, 105(4), 1233-1243.

Deckers J., De Koninck R., Bos S., Broothaers M., Dirix K., Hambsch L., Lagrou, D., Lanckacker T., Matthijs, J., Rombaut B., Van Baelen K., and Van Haren T., 2019. Geologisch (G3D) en hydrogeologisch (H3D) 3D-lagenmodel van Vlaanderen – versie 3. Studie uitgevoerd in opdracht van het Vlaams Planbureau voor Omgeving, departement Omgeving en de Vlaamse Milieumaatschappij. VITO-rapport 2018/RMA/R/1569.

Deckers, J., and Van der Voet, E., 2018. A review on the structural styles of deformation during Late Cretaceous and Paleocene tectonic phases in the southern North Sea area. J. Geodyn., 115, 1–9.

Deckers, J., Van Noten, K., Schiltz, M., Lecocq, T., and Vanneste, K., 2018. Integrated study on the topographic and shallow subsurface expression of the Grote Brogel Fault at the boundary of the Roer Valley Graben, Belgium. Tectonophysics, 722, 486-506.

Deckers, J., Vernes, R., Dabekaussen, W., Den Dulk, M., Doornenbal, H., Dusar, M., Matthijs, J., Menkovic, A., Reindersma, R., Walstra, J., Westerhoff, W., and Witmans, N., 2014. Geologisch en hydrogeologisch 3D model van het Cenozoïcum van de Roerdalslenk in Zuidoost-Nederland en Vlaanderen (H3O-Roerdalslenk). VITO-rapport, 2014/ETE/R/1, 200 pp.

De Jager, J., 2003. Inverted basins in the Netherlands, similarities and differences, Neth. J. Geosci., 82(4), 355–366.

Demyttenaere, R., 1989. The post-Paleozoic geological history of north-eastern Belgium. In: Mededelingen van de Koninklijke Academie voor Wetenschappen, Letteren en Schone Kunsten van België, 51, 51–81.

Demyttenaere, R., and Laga, P.G., 1988. Breuken- en isohypsenkaarten van het Belgisch gedeelte van de Roerdalslenk: eerste resultaten van een seismisch onderzoek in het gebied Poppel-Lommel-Maaseik. In: Ministerie van Economische Zaken, Administratie der Mijnen. België, Brussels, Geologische Dienst van België.

Duin, E.J.T., Doornenbal, J.C., Rijkers, R.H.B., Verbeek, J.W., and Wong, T.E., 2006. Subsurface structure of the Netherlands—results of recent onshore and offshore mapping. Neth. J. Geosci., 85, 245–276.

Ebinger, C., and Casey, M., 2001. Continental breakup in magmatic provinces: an Ethiopian example. Geology, 29, 527–530.

Everaerts, M., and De Vos, W., 2012. Gravity acquisition in Belgium and the resulting Bouguer anomaly map. Mem. Geol. Surv. Belgium, 58, 39 p.

Geluk, M.C., 1990. The Cenozoic Roer Valley Graben, Southern Netherlands. Meded Rijks Geol Dienst, 44, 65–72.

Geluk, M.C., Duin, E.J., Dusar, M., Rijkers, R.H., van den Berg, M.W., and van Rooijen, P., 1994. Stratigraphy and tectonics of the Roer Valley Graben. Geol. Mijnb., 73, 129–141.

Katumwehe, A.B., Abdelsalam, M.G., and Atekwana, E.A., 2015. The role of pre-existing Precambrian structures in rift evolution: the Albertine and Rhino grabens, Uganda. Tectonophysics, 646, 117–129.

Kendall, J.M., Stuart, G.W., Ebinger, C.J., Bastow, I.D., and Keir, D., 2005. Magma-assisted rifting in Ethiopia. Nature, 433, 146–148

Kockel, F., 2003. Inversion structures in central Europe—Expressions and reasons, an open discussion, Neth. J. Geosci., 82(4), 367–382.

Langenaeker, V., 2000. The Campine Basin: stratigraphy, structural geology, coalification and hydrocarbon potential for the Devonian to Jurassic. Aardkundige Mededelingen, 10, 1–142.

Luijendijk, E., Van Balen, R.T., Ter Voorde, M. and Andriessen, P.A.M., 2011. Reconstructing the Late Cretaceous inversion of the Roer Valley Graben (southern Netherlands) using a new model that integrates burial and provenance history with fission track thermochronology. Journal of Geophysical Research, 116, B06402.

Matthijs, J., Lanckacker, T., De Koninck, R., Deckers, J., Lagrou, D. and Broothaers, M., 2013. Geologisch 3D lagenmodel van Vlaanderen en het Brussels Hoofdstedelijk Gewest - versie 2, G3Dv2. Studie uitgevoerd door VITO in opdracht van de Vlaamse overheid, Departement Leefmilieu, Natuur en Energie, Afdeling Land en Bodembescherming, Ondergrond, Natuurlijke Rijkdommen, VITO-rapport 2013/R/ETE/43.

McClay, K.R., and Buchanan, P.G., 1992. Thrust faults in inverted extensional basins. In: McClay, K.R., (Ed), Thrust Tectonics, 93-104.

Meyus,Y., Cools, J., Adyns, D., Zeleke, S.Y., Woldeamlak, S.T., Batelaan, O., and De Smedt, F., 2005. Hydrogeologische detailstudie van de ondergrond in Vlaanderen. Eindrapport. Ministerie van de Vlaamse Gemeenschap, Administratie Milieu-, Natuur-, Land- en Waterbeheer, Afdeling Water, 107 pp. + bijlagen.

Michon, L., and Van Balen, R.T., 2005. Characterization and quantification of active faulting in the Roer valley rift system based on high precision digital elevation models. Quat. Sci. Rev., 24, 457–474.

Michon, L., Van Balen, R.T., Merle, O., and Pagnier, H., 2003. The Cenozoic evolution of the Roer Valley Rift system integrated at a European scale. Tectonophysics, 367, 101–126.

Mora, A., Gaona, T., Kley, J., Montoya, D., Parra, M., Quiroz, L.I., Reyes, G., and Strecker, M.R., 2009. The role of inherited extensional fault segmentation and linkage in contractional orogenesis: a reconstruction of lower cretaceous inverted rift basins in the eastern cordillera of Colombia. Basin Res., 21, 111-137.

Mora, A., Parra, M., Strecker, M.R., Kammer, A., Dimaté, C., and Rodriguez, F., 2006. Cenozoic contractional reactivation of Mesozoic extensional structures in the Eastern Cordillera of Colombia. Tectonics, 25, TC2010

Nixon, C. W., Bull, J. M., and Sanderson, D. J., 2014. Localized vs distributed deformation associated with the linkage history of an active normal fault, Whakatane Graben, New Zealand: Journal of Structural Geology, 69, p. 266-280.

Paulissen, E., 1997. Quaternary morphotectonics in the Belgian part of the Roer Graben. In: Aardkundige Mededelingen, 8, 131–134.

Rypens, J., Sintubin, M., and Dusar, M., 2004. Geometry and kinematics of the southwestern border fault system of the Roer Valley Graben (NE Belgium). KU Leuven and Belgische Geologische Dienst, p 86.

Sels, O., Claes, S., and Gullentops, F., 2001. Toelichtingen bij de Geologische kaart van België Vlaams Gewest 1 :50.000, Kaartblad 18-10 Maaseik + Beverbeek. Belgische Geologische Dienst en Ministerie van de Vlaamse Gemeenschap, Afdeling Natuurlijke Rijkdommen en Energie, Brussel.

Soliva, R., and Schultz, R.A., 2008. Distributed and localized faulting in extensional settings: Insight from the North Ethiopian RifteAfar transition area. Tectonics, 27, TC2003.

Verbeurgt, J., Camp, M. Van, Stal, C., Camelbeeck, T., Sloover, L. De, Poppe, H., Declercq, P.Y., Voet, P., Constales, D., Troch, P., De Maeyer, P., and De Wulf, A., 2019. The gravity database for Belgium. Geosci. Data J., 6, 116-125.

Vernes, R.W., Deckers, J., Bakker, M.A.J., Bogemans, F., De Ceukelaire, M., Doornenbal, J.C., den Dulk, M., Dusar, M., Van Haren, T.F.M., Heyvaert, V.M.A., Kiden, P., Kruisselbrink, A.F., Lanckacker, T., Menkovic, A., Meyvis, B., Munsterman, D.K., Reindersma, R., ten Veen, J.H., van de Ven, T.J.M., Walstra, J., and Witmans, N., 2018. Geologisch en hydrogeologisch 3D model van het Cenozoïcum van de Belgisch-Nederlandse grensstreek van Midden-Brabant / De Kempen (H3O – De Kempen). Studie uitgevoerd door VITO, TNO-Geologische Dienst Nederland en de Belgische Geologische Dienst in opdracht van Vlaams Planbureau voor Omgeving, Vlaamse Milieumaatschappij, TNO, Geologische Dienst Nederland, Nederlandse Provincie Noord-Brabant, Brabant Water, Programmabureau KRW/DHZ Maasregio.

Wright, T.J., Ebinger, C., Biggs, J., Ayele, A., Yirgu, G., Keir, D., and Stork, A., 2006. Magmamaintained rift segmentation at continental rupture in the 2005 Afar dyking episode. Nature, 442, 291–294.

Worum, G., Michon, L., van Balen, R. T., van Wees, J.-D., Cloetingh, S., and Pagnier, H., 2005. Pre-Neogene controls on present-day fault activity in the West Netherlands Basin and Roer Valley Rift System (southern Netherlands): role of variations in fault orientation in a uniform low-stress regime: Quaternary Science Reviews, 24(3-4), p. 473-488.

Ziegler PA, 1988. Evolution of the Artic North Atlantic and the western Tethys. Am. Assoc. Pet. Geol. Mem., 43, 198 pp..

https://doi.org/10.5194/se-2020-23
Preprint. Discussion started: 9 March 2020

Figures

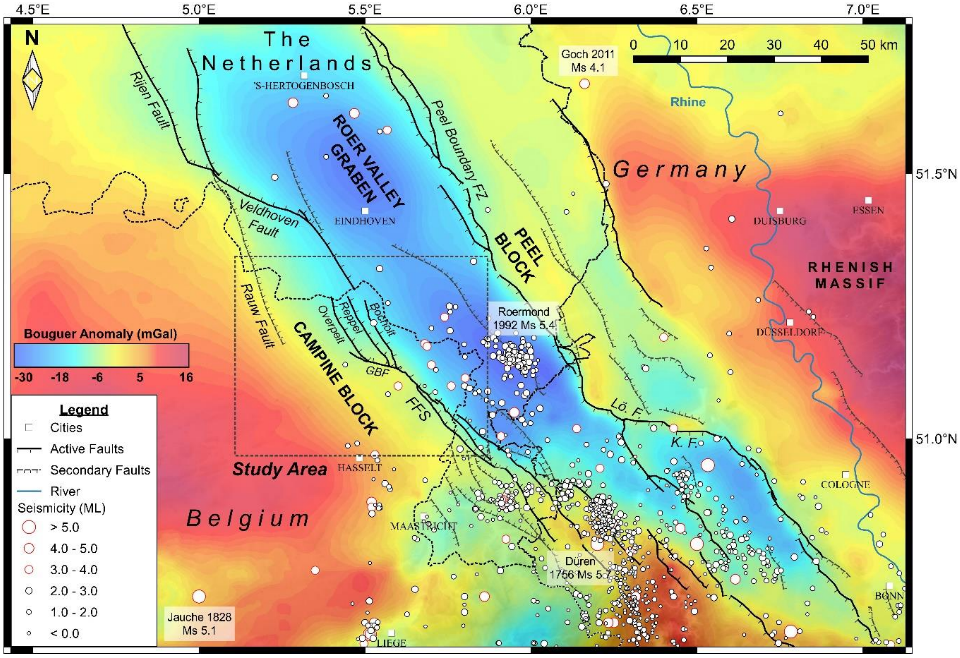

Fig. 1: Roer Valley Graben (RVG) border fault configuration and seismicity in relation to the Bouguer anomaly. Note the lower Bouguer Anomaly values (Bouguer data gathered by the ROB as described in Everaerts & De Vos, 2012 and Verbeurgt et al., 2019) in the RVG related to the thick Cenozoic sequence of uncompacted sediments. The grey dashed square indicates the study area and the location of Figs. 3, 4 and 5. Lö. F.: Lövenich Fault; K. F.: Kast Fault. Coordinates in WGS84. Surface fault traces 634 modified after Vanneste et al. (2013) and Deckers et al. (2018). Historical and instrumental natural 635 seismicity updated until Dec. 2019 (ROB catalog, 1350-2019).

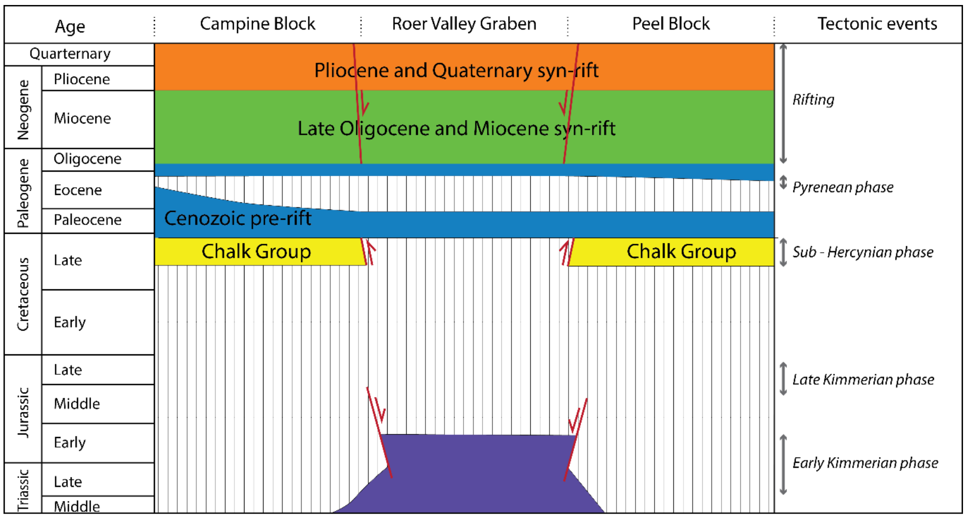

Fig. 2: General stratigraphy, ages and the main tectonic phases within the Campine Block, Roer Valley Graben and Peel Block. This figure was modified after Geluk et al. (1994).

https://doi.org/10.5194/se-2020-23
Preprint. Discussion started: 9 March 2020

Solid Earth
Discussions

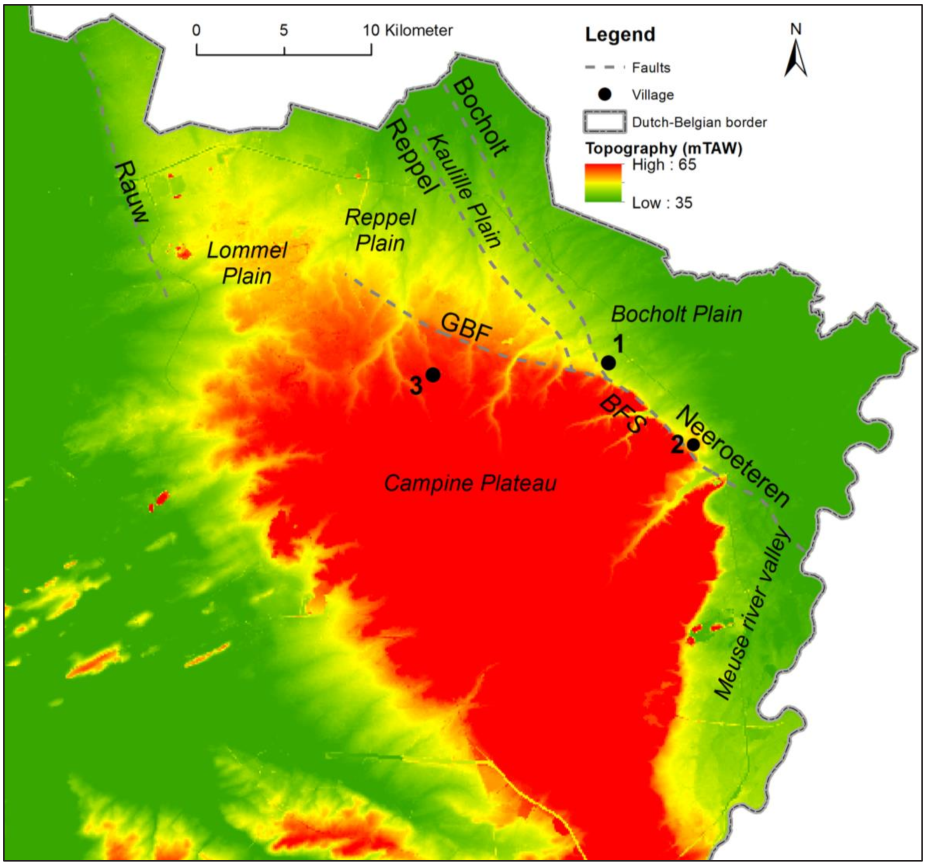

Fig. 3: Topography in the study area with indication of the main morphological features and faults of the G3Dv3-model that have a topographic expression. BFS= Bree Fault Scarp; GBF = Grote Brogel fault; Numbers denote villages: 1 = Bree; 2 = Waterloos; 3 = Peer. DTMv2 model from Agentschap Informatie Vlaanderen (2018).

https://doi.org/10.5194/se-2020-23
Preprint. Discussion started: 9 March 2020

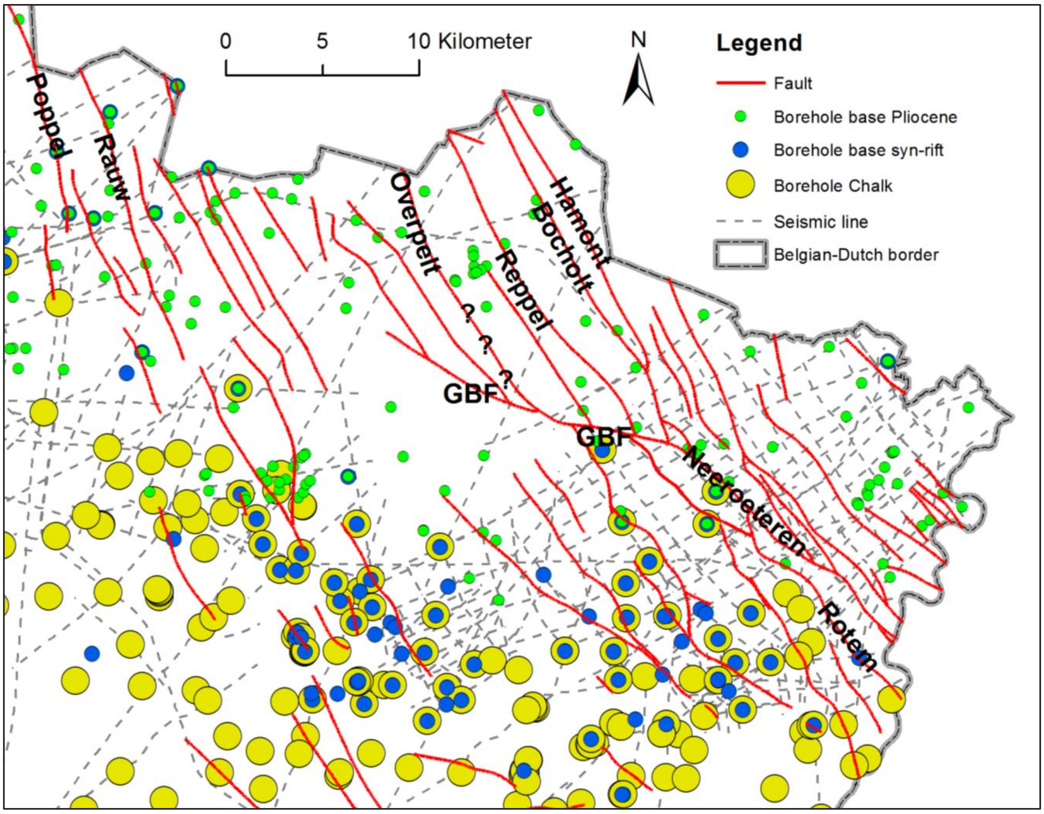

Fig. 4: Overview map of the main input-data used for the G3Dv3-model of the area, namely seismic lines and borehole selections (for mapping of the bases of the Pliocene, syn-rift strata and Chalk Group). The modelled fault lines in the base syn-rift strata and the major one in the Chalk Group are also shown. Note the difference in seismic coverage of the northern and southern study areas.

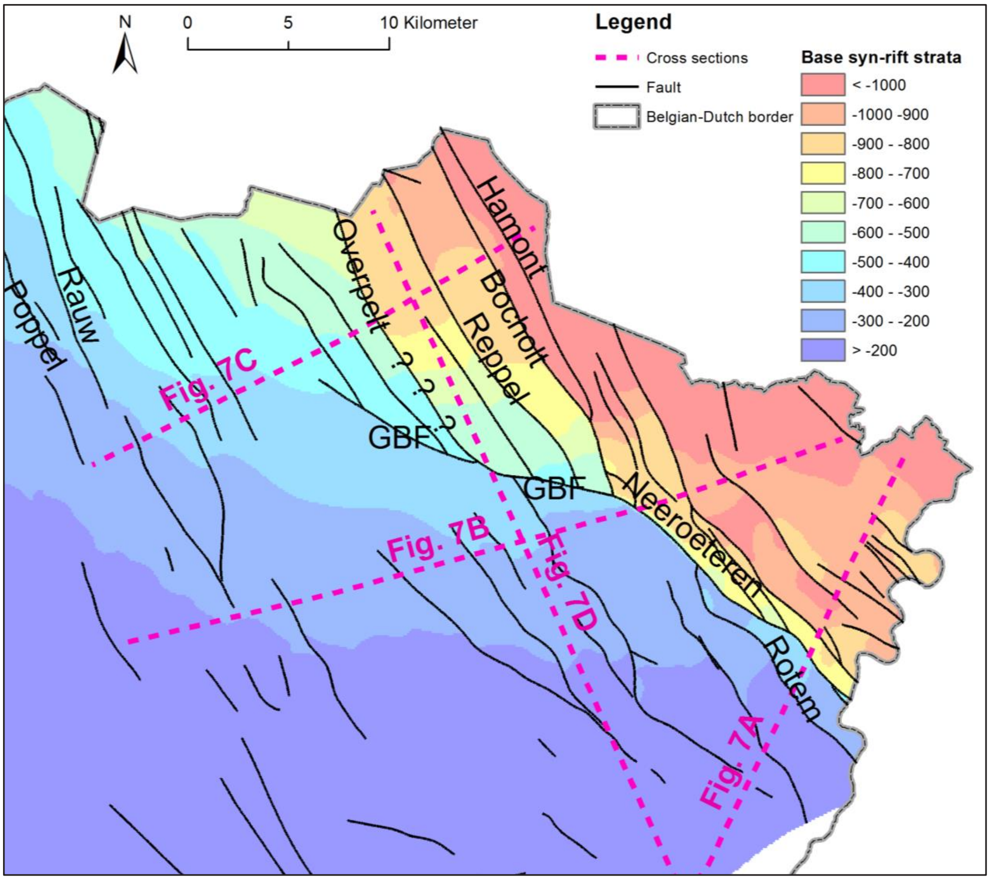

Fig. 5: Map showing the depth of the base of the syn-rift strata and the syn-rift faults in the study area from the G3Dv3-model. The locations of the cross-sections in figure 7 are also indicated.

https://doi.org/10.5194/se-2020-23
Preprint. Discussion started: 9 March 2020

Solid Earth Discussions
Open Access

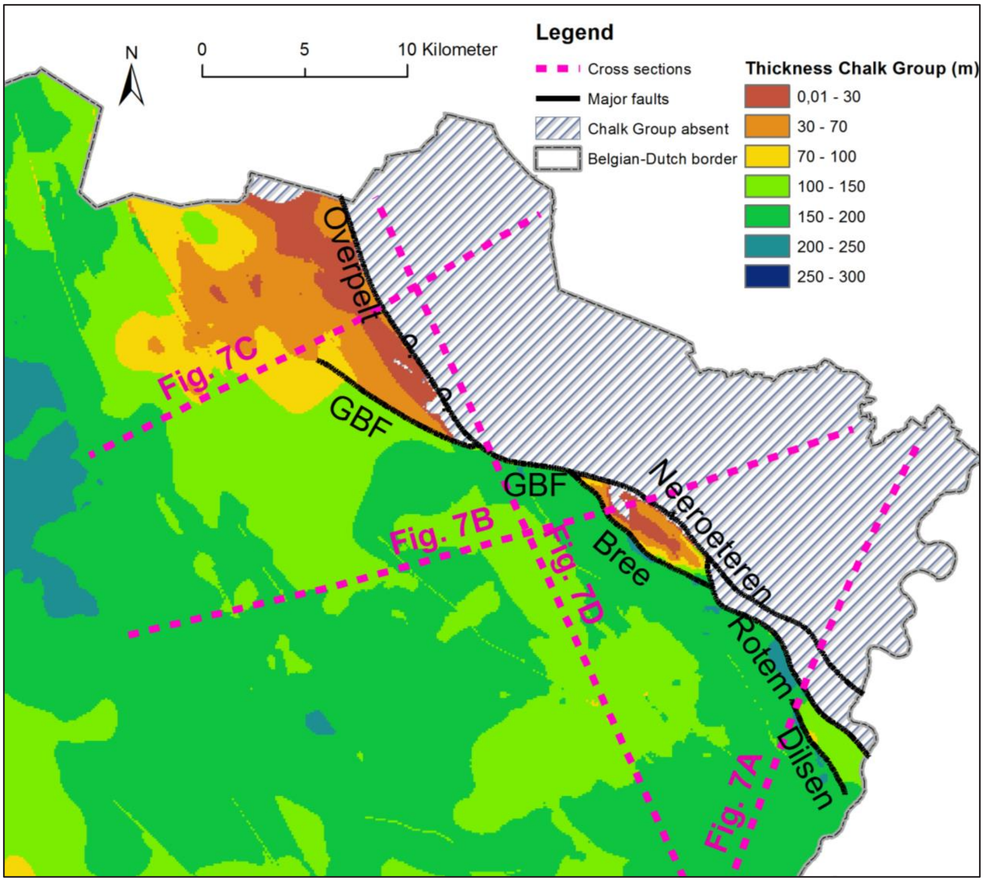

Fig. 6: Map showing the thickness of the Chalk Group and major reverse/thrust faults that influenced it in the study area from the G3Dv3-model. The locations of the cross-sections in figure 7 are also indicated. Note that our informal definition of the Chalk Group only contains those parts of the formal Chalk Group that were deposited during inversion of the RVG, and are therefore missing in the latter. Younger formations of the formal Chalk Group are placed in the Cenozoic pre-rift strata for the purpose of this study.

https://doi.org/10.5194/se-2020-23
Preprint. Discussion started: 9 March 2020

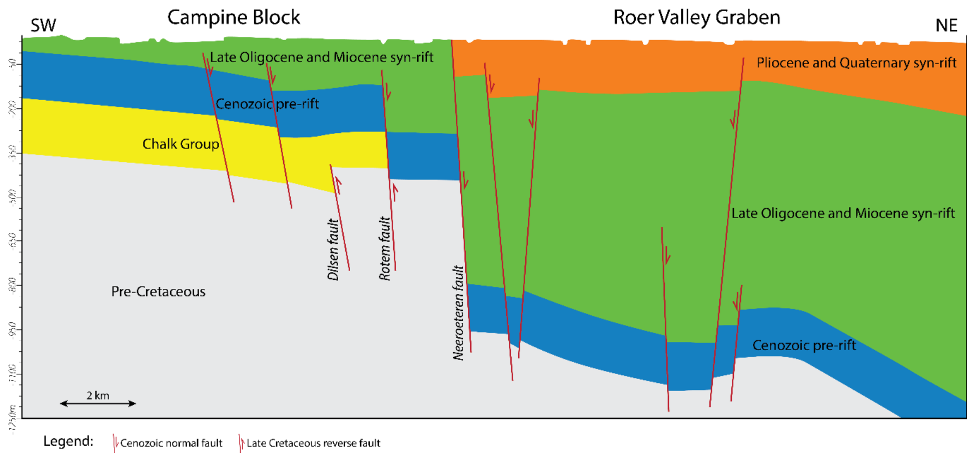

Fig. 7A. Section A constructed from the G3Dv3-model across the southern domain of the FFS. For location of this section, see figures 5 and 6. During both Cenozoic extension and late Cretaceous compression, this domain was dominated by large vertical throws along the border faults. Consequently, this domain of the FFS is rather narrow. The Dilsen fault was an important thrust fault during late Cretaceous compression, but inactive during Cenozoic rifting, whereas the Rotem fault was active during both phases.

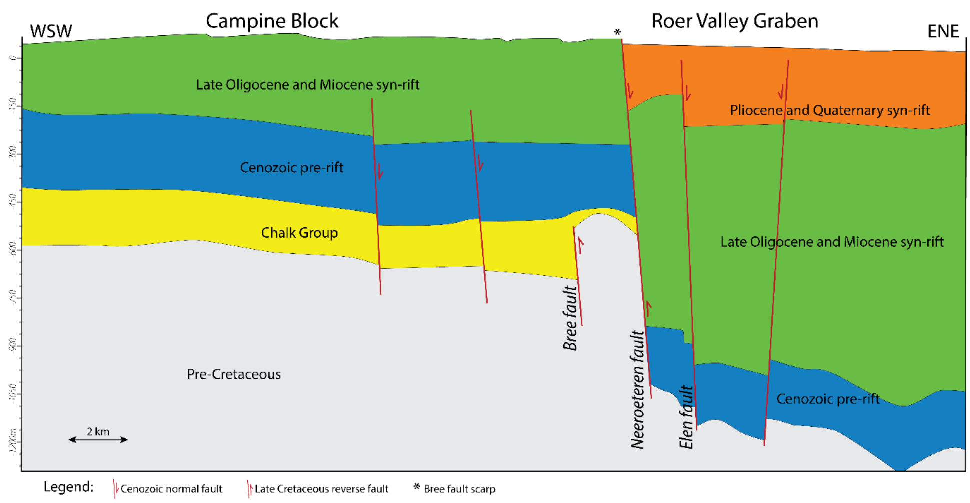

Fig. 7B. Section B constructed from the G3Dv3-model across the southern domain of the FFS. For location of this section, see figures 5 and 6. During both Cenozoic extension and late Cretaceous compression, this domain was dominated by large vertical throws along the border faults. Consequently, this domain of the FFS is rather narrow. The Bree Uplift was important during late Cretaceous compression, but inactive during Cenozoic rifting. Similar to figure 7A, almost all Cenozoic extension was accommodated by the large vertical throw along the Neeroeteren fault.

https://doi.org/10.5194/se-2020-23
Preprint. Discussion started: 9 March 2020

Solid Earth Discussions

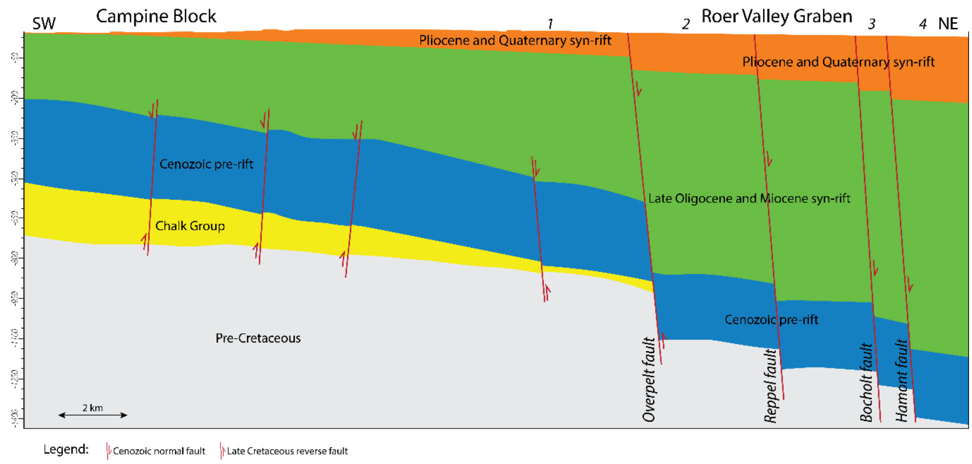

Fig. 7C. Section C constructed from the G3Dv3-model across the northern domain of the FFS. For location of this section, see figures 5 and 6. During both Cenozoic extension and late Cretaceous compression, this domain was dominated in the west by flexural movements rather than strong vertical fault throws. Consequently, this domain of the FFS is relatively wide compared to the southern domain of the FFS in figures 7A and 7B. 1= Lommel Plain; 2= Reppel Plain; 3= Kaulille Plain; 4= Bocholt Plain.

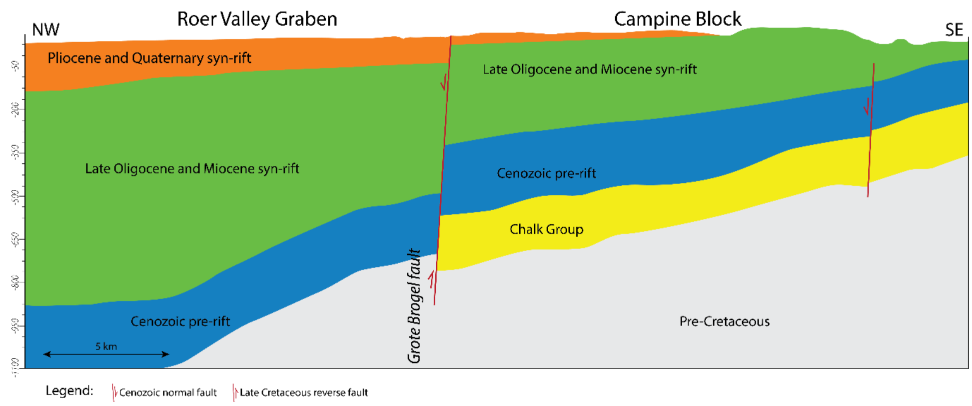

Fig. 7D. Section D constructed from the G3Dv3-model from the footwall of the southern domain of the FFS (southeast of the GBF) into the hangingwall of the northern domain of the FFS (northwest of the GBF). For location of this section, see figures 5 and 6. Note how the thickness of the syn-rift strata gradually increases in northern direction, with a strong jump across the GBF. The thickness of the Chalk Group on the other hand remains more or less uniform in the south and becomes absent in the hangingwall to the GBF into the northern domain of the FFS.